COMMUNICATION

Hemicubane topological analogs of the oxygen-evolving complex of photosystem II mediating water-assisted propylene carbonate oxidation

Received 00th January 20xx, Accepted 00th January 20xx

DOI: 10.1039/x0xx00000x

Connor A. Koellner, a Michael R. Gau, b Aleksander Polyak, a Manish Bayana, a Michael J. Zdilla*

A series of Ca-Mn clusters with the ligand 2-pyridinemethoxide (Py- CH_2O) have been prepared with varying degrees of topological similarity to the biological oxygen-evolving complex. These clusters activate water as a substrate in the oxidative degradation of propylene carbonate, with activity correlated with topological similarity to the OEC, lowering the onset potential of the oxidation by as much as 700 mV.

Photosynthetic organisms have evolved to harness sunlight to transform water and carbon dioxide precursors into complex carbohydrates and dioxygen. Photosystem II (PSII), a multisubunit membrane protein present in all oxygenic photosynthetic organisms, is responsible for the initial step of the photosynthetic electron transfer pathway. The active site of this photoenzyme, the oxygen-evolving complex (OEC) (Figure 1), is responsible for water oxidation, and has been identified as a $CaMn_4O_n$ cubane cluster that is able to catalyze biological water splitting. $^{1-7}$

The OEC consists of four manganese ions and a calcium ion, arranged as a distorted Mn₃Ca heterocubane with an additional pendant Mn-O arm, as shown in Figure 1.^{4,8} Calcium also binds water, and is an integral part of the OEC and required for water oxidation catalysis to transpire, and only Sr may substitute Ca (giving a fraction of the activity).^{9, 10} Thus, inclusion of Ca in synthetic models is a priority. However, most functional models¹¹⁻²⁰ of the OEC do not have biomimetic topology, and most molecular topological mimics²¹⁻²⁵ do not show biomimetic chemistry, with some exceptions.²⁶⁻⁴³

Electrochemistry is an oft-employed tool for investigation of catalytic water oxidation by biomimetic systems. ^{13, 26, 34, 43} An example particularly germane to this report is the oxidation of water to hydrogen peroxide by a manganese cluster from

Presented here is the synthesis and characterization of a series of OEC structural models with hemicubane geometry (i.e., a heterocubane structure minus one corner metal ion) derived from self-assembled precursor fragments. These clusters represent near topological analogues of the OEC; in particular, the compound $CaMn_3(PyCH_2O)_6(NR_2)_2(THF)$ (2) has an identical core atom arrangement but for the absence of one Mn atom (Figure 1). The synthesis, characterization, and electrocatalytic water activation chemistry is presented.

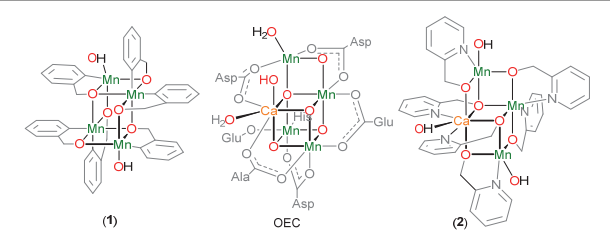


Figure 1. Structural comparison between the OEC (center) and NR₂-hydrolyzed products of compounds featured in this report. Structure **1** lacks the Ca ion, and the analogous "dangler" atom is oriented away from the viewer. **2** is even more similar, with only a back-corner Mn missing from the topological analogy.

The synthetic procedures employed are designed to provide Mn and Ca precursors in desired ratios by addition of $Ca(NR_2)_2$ and $Mn(NR_2)_2$ at (or close to) the ratio present in the final product. The array of characterized products is summarized in Scheme 1. We have found (as is often the case in self-assembly chemistry) that the best results are sometimes obtained when the stoichiometry of metal precursors is slightly different from that of metals in the final product. In this case, we found that a slight excess of 2-pyridine methanol does not necessarily result in complete protolysis of NR_2 ligands, as one might expect, but instead, gives good purity products since reactivity typically ceases with displacement of all but two remaining terminal NR_2 -ligands (presumably sterically inaccessible to additional equivalents of $PyCH_2OH$). For example, $Mn_4(PyCH_2O)_6(NR_2)_2$ (1)

Agapie. This reaction was carried out in a propylene carbonate/water co-solvent system.¹³ The catalyst is non-cuboid, but possesses a biomimetic pendant metal moiety.

a. Department of Chemistry, Temple University, Philadelphia PA 19086

b Department of Chemistry, University of Pennsylvania, Philadelphia PA 19104 Electronic Supplementary Information (ESI) available: Experimental, additional discussion of electrochemical experiments and figures, EPR, UV-Visible, and IR spectra, and crystallographic tables. Crystallographic information files (CIF) are also available from the CCDC under deposition numbers 2032641-203264. See DOI: 10.1039/x0xx00000x

COMMUNICATION Journal Name

is prepared from a 2.5:1 ratio of $PyCH_2OH$ to $Mn(NR_2)_2$, even though the final product has a ligand:metal ratio of only 1.5:1, and the final product retains two unprotolyzed amido ligands, implying unincorporated equivalents of excess $PyCH_2OH$, and implicating the following stoichiometry:

^{THF}
4 Mn(NR₂)₂ + 6 PyCH₂OH →
$$Mn_4(PyCH_2O)_6(NR_2)_2 (1) + 6 HNR_2$$
 (1)

Cluster 1 is an edge-fused double hemicubane cluster with four ligand oxygen atoms acting as μ_2 -bridging ligands and two as μ_3 bridging ligands (Figure 2). Charge counting considerations indicate that the compound is all-Mn^{II}. Maintenance of the divalent state is expected from the energetically gentle protolytic synthesis. The EPR spectrum of 1 (and 2-4, vide infra) is a broad $S = \frac{5}{2}$ signature consistent with paramagnetic (i.e., randomly oriented) Mn $\frac{5}{2}$ centers (Figure S1). The absence of d-electronic transitions in the UV-Visible spectra (Figure S2) further supports the assignment of high-spin d⁵ Mn^{II} systems. The cluster possesses topological analogy to the OEC, but is missing the Ca ion. The cluster features 5-coordinate manganese at the termini (uncommon for Mn-O clusters, which are mostly 6-coordinate⁴⁴), presumably controlled by the steric encumbrance imposed by the bulky NR2 ligands. The combination of an open coordination site on Mn and a hydrolyzable NR2 ligand is expected to facilitate water binding at manganese, a prerequisite for water activation chemistry.

With regard to metal stoichiometry, in the case of mixed Ca/Mn cluster synthesis, we have found it is advantageous to have a slight excess of $Mn(NR_2)$ in order to get high-quality crystals of uniform morphology and good purity. The stoichiometries of metals in the products of the reaction demonstrate that $Ca(NR_2)_2$ is more reactive toward protolysis

than $Mn(NR_2)_2$. This is expected since the Mn-N bond is more covalent, making the bonding electron pair less available for protonation than that of the ionic Ca-N contacts, making the NR_2 ligand at Ca much more Brønsted basic than that at Mn. In the synthesis of cluster $\bf 2$, which possesses a 1:3 ratio of Ca:Mn, the synthesis is performed using a 1:5 ratio of Ca:Mn. As the Ca reacts most rapidly (but is limiting), the resulting compound incorporates a single calcium ion, presumably leaving behind unincorporated Mn species which contaminate the mixture, and which are removed during crystallization:

The structure of the core of ${\bf 2}$ is essentially equivalent to that of ${\bf 1}$, but with a single manganese replaced by a THF-ligated, 7-coordinate calcium ion (Figure 2). The presence of the labile THF at Ca, coordinative unsaturation, and hydrolyzable NR₂ ligands at Mn denotes high probability of biomimetic water binding at Mn and/or Ca when exposed to water. Due to the propensity of self-assembly chemistry to form mixtures of products, obtaining high-purity material is a challenge in general. However, this approach of including excess Mn(NR₂)₂ equivalents appears to favor the insertion of a single calcium ion by virtue of the more reactive Ca(NR₂)₂ to give ${\bf 2}$ in good purity based on CHN combustion analysis. Similar to ${\bf 1}$, the core of ${\bf 2}$ is a corner-voided analogue of the OEC, similar but for a missing Mn²⁺ ion, whereas in ${\bf 1}$, the missing atom is Ca. (Figure 1).

The tetranuclear cluster geometries of **1** and **2** are related to the geometry of the previously reported all-cobalt hemicubane water oxidation catalyst of Xie et al, which makes use of a similar N-methanol-3,5-dimethylpyrazole ligand. ⁴⁵ In our work, this geometry appears to be characteristic of only the all-Mn and the 1:3 Ca:Mn clusters only, as deviations from this Ca-Mn ratio leads to cluster expansion. When the ratio of Ca to Mn synthetic precursors is further decreased from 1:5 to 1:8, rather than obtaining a mixture of **1** and **2**, an expanded cluster, CaMn₅(PyCH₂O)₁₀(NR₂)₂ (**3**, Figure 3) results, forming according to the following stoichiometry:

5 Mn(NR₂)₂ + 1 Ca(NR₂)₂ + 10 PyCH₂OH →
$$CaMn_5(PyCH_2O)_{10}(NR_2)_2 (3) + 10 HNR_2 (3)$$

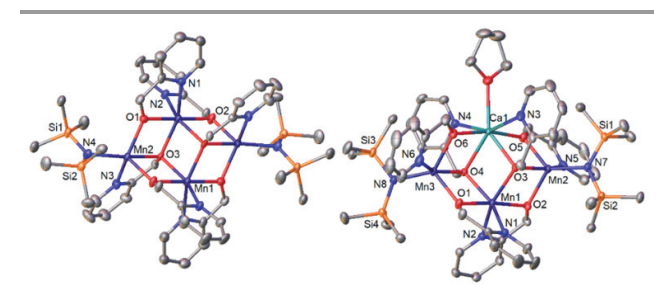


Figure 2. Thermal ellipsoid plot of $1\cdot0.5$ THF (top) and $2\cdot$ THF (bottom). Ellipsoids set at 50% probability level. Hydrogens omitted and carbon atoms shown in stick mode for clarity. THF solvate not shown.

Journal Name COMMUNICATION

The structure of **3** is analogous to that of **2**, containing edge-fused hemicubanes with 5-coordinate terminal manganese atoms, but is extended by two additional $Mn(PyCH_2O)_2$ formula units, adding a third and fourth hemicubane feature. Additionally, the extension of the cluster by two $Mn(PyCH_2O)_2$ units increases the quantity of interior 2-pyridinemethoxide ligands, which preferentially ligate calcium, resulting in an 8-coordinate center.

The reaction performed with a larger 1:2 ratio of Ca:Mn results in the formation of $Ca_2Mn_4(PyCH_2O)_{10}(NR_2)_2$ (4), a cluster essentially equivalent to 3, but with the replacement of the other central Mn ion with Ca:

The structure of **4** (Figure 3) is similar to that of **3** but for the replacement of the other central Mn with Ca. Further, a pyridine group has migrated from the 8-coordinate calcium to the new calcium site, making both calcium centers 7-coordinate in **4**.

Finally, if Ca and Mn precursors are combined in a ratio of unity, isolated is a cationic cluster $[Ca_4Mn_3(PyCH_2O)_{12}(THF)_6]^{2+}$, (5, Figure 4), a star-shaped cluster of six edge-fused hemicubane features. The counterions are the well-known⁴⁶⁻⁵⁰ tris[bis(trimethylsilyI)amido]manganate(II) anionic complex:

5 Mn(NR₂)₂ + 4 Ca(NR₂)₂ + 12 PyCH₂OH
$$\rightarrow$$
 [Ca₄Mn₃(PyCH₂O)₁₂(THF)₆][Mn(NR₂)₃]₂ (**5**) + 12 HNR₂ (5)

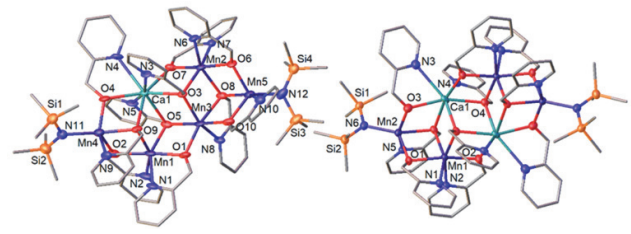


Figure 3. Thermal ellipsoid plot of 3.7 THF (top) and 4.5.25 THF (bottom). Ellipsoids set at 50% probability level. Hydrogens omitted, THF solvate not shown, and carbon atoms shown in stick mode for clarity.

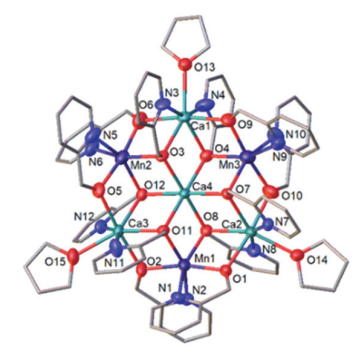


Figure 4. Thermal ellipsoid plot of [5]²⁺ cation of [5][Mn(N(SiMe₃)₂)₃]₂·4.5 THF. Ellipsoids set at 50% probability level. Hydrogen, THF solvate, and [Mn(NR₂)₃] anions omitted, and carbon atoms shown in stick mode for clarity.

It bears noting that complex **5** bears an identical core structure to the all-cobalt water oxidizing cluster of Xu et al. 35 Unlike complexes **1-4**, the EPR of **5** is fairly complex, showing at least three apparent signals (Figure S1). The g = 2 signal exhibits hyperfine coupling, and is assigned to the anionic [Mn(NR₂)₃] anions due to the six-line hyperfine signal and the expected appearance of an S = 5/2 broad g = 2 feature for Mn^{II}. There is additionally a sharp g = 4 rhombic signal tentatively assigned to an S = 3/2 or 5/2 state of **5**, and which bears some resemblance to the g = 4 signal of PSII⁵¹. There is a third broad signal with a large degree of zero-field splitting evidenced by the appearance of at least one satellite signal at g = 10. This may represent an alternative spin state of **5**, or an equilibrium isomer.

Of interest for any OEC topological model is electrochemical water activation. Since 1-5 are insoluble in water, we explored the use of propylene carbonate as a co-solvent to its electrochemical robustness, decomposing only above 1.5 V vs. NHE (Figure S3), which makes it of utility as an electrolyte in high-voltage lithium batteries.⁵² In the absence of water, compounds 1-5 all exhibit fairly featureless cyclic voltammograms, suggesting manganese(II) in this ligand template is stable to reduction even to -2 V vs, and to oxidation up to beyond 1V NHE. (Figure S4). Addition of 1-3% water results to the catalyst solutions does not result in formation of any solid, but, as shown in Figure S5, a catalytic current is observed during an anodic sweep for clusters 2-4 (those most topologically related to the OEC). The catalytic current is proportional to water concentration (Figure S6), implicating the involvement of water in the catalytic process. Analysis of the head space of the reaction by gas chromatography (Figure S10) reveals no formation of O2, and CO2 as the sole detected gaseous byproduct. Control experiments in the absence of water reveal that the catalytic current is too large to be attributable to ligand oxidation, thus implicating water-assisted solvent decomposition as the reaction responsible for the catalytic current. Repeat scans and chronoamperometry on compounds 2-4 (Figure S9) were performed, and rule out the possibility that a solid or nano-phase metal oxide is responsible for the catalytic reaction by 3 and 4, though 2 exhibits some current growth during chronoamperometry, suggesting the possibility of catalyst deposition at the electrode (see Supporting Information).

Presented is a series of biologically inspired OEC topological analogues that electrochemically activate water for the anodic decomposition of the electrochemically robust propylene carbonate molecule. A correlation between activity and structural analogy to the OEC is unmistakable, with the most active catalysts being close topological analogues. Compound 2, for instance, exhibits a similar cluster core to the OEC minus one manganese atom (Figure 1). The strict requirement for Ca²⁺ in these catalysts as well as the rate dependence on water implicate the activation of a water molecule by calcium to mediate the chemistry. Future work on these cluster systems will seek to functionalize the ligands with polar or charged groups to facilitate water solubility, so that electrocatalysis may be explored in greater concentrations of water so that the possibility of direct water oxidation may be investigated.

COMMUNICATION Journal Name

Conflicts of interest

There are no conflicts to declare

Notes and references

- H. Dau, I. Zaharieva and M. Haumann, Curr. Opin. Chem. Biol., 2012, 16, 3-10.
- M. Askerka, G. W. Brudvig and V. S. Batista, Acc. Chem. Res., 2017, 50, 41-48.
- J. P. McEvoy and G. W. Brudvig, Chem. Rev., 2006, 106, 4455-4483.
- M. Suga, F. Akita, K. Hirata, G. Ueno, H. Murakami, Y. Nakajima, T. Shimizu, K. Yamashita, M. Yamamoto, H. Ago and J.-R. Shen, Nature, 2015, 517, 99-103.
- A. Tanaka, Y. Fukushima and N. Kamiya, J. Am. Chem. Soc., 2017, 139, 1718-1721.
- 6. J. Yano and V. Yachandra, Chem. Rev., 2014, 114, 4175-4205.
- 7. D. J. Vinyard, G. M. Ananyev and G. C. Dismukes, *Ann. Rev. Biochem.*, 2013, **82**, 577-606.
- Y. Umena, K. Kawakami, J.-R. Shen and N. Kamiya, *Nature*, 2011, 473, 55-60.
- F. H. M. Koua, Y. Umena, K. Kawakami and J.-R. Shen, *Proc. Natl. Acad. Sci. USA*, 2013, **110**, 3889.
- A. Boussac, F. Rappaport, P. Carrier, J.-M. Verbavatz, R. Gobin,
 D. Kirilovsky, A. W. Rutherford and M. Sugiura, J. Biol. Chem.,
 2004, 279, 22809-22819.
- 11. J. Limburg, J. S. Vrettos, L. M. Liable-Sands, A. L. Rheingold, R. H. Crabtree and G. W. Brudvig, *Science*, 1999, **283**, 1524-1527.
- R. Al-Oweini, A. Sartorel, B. S. Bassil, M. Natali, S. Berardi, F. Scandola, U. Kortz and M. Bonchio, *Angew. Chem. Int. Ed.*, 2014, 53, 11182-11185.
- Z. Han, K. T. Horak, H. B. Lee and T. Agapie, J. Am. Chem. Soc., 2017, 139, 9108-9111.
- 14. Y. Gao, T. r. Åkermark, J. Liu, L. Sun and B. r. Åkermark, *J. Am. Chem. Soc.*, 2009, **131**, 8726-8727.
- 15. H. Chen, R. Tagore, S. Das, C. Incarvito, J. W. Faller, R. H. Crabtree and G. W. Brudvig, *Inorg. Chem.*, 2005, **44**, 7661-7670.
- 16. Y. Gao, R. H. Crabtree and G. W. Brudvig, *Inorg. Chem.*, 2012, **51**, 4043-4050.
- M. Hirahara, A. Shoji and M. Yagi, *Eur. J. Inorg. Chem.*, 2014, 2014, 595-606.
- 18. L. Ma, Q. Wang, W.-L. Man, H.-K. Kwong, C.-C. Ko and T.-C. Lau, *Angew. Chem. Int. Ed.*, 2015, **54**, 5246-5249.
- K. J. Young, M. K. Takase and G. W. Brudvig, *Inorg. Chem.*, 2013, 52, 7615-7622.
- 20. W.-T. Lee, S. B. Muñoz, D. A. Dickie and J. M. Smith, *Angew. Chem. Int. Ed.*, 2014, **53**, 9856-9859.
- 21. J. S. Kanady, E. Y. Tsui, M. W. Day and T. Agapie, *Science*, 2011, **333**, 733-736.
- S. Mukherjee, J. A. Stull, J. Yano, T. C. Stamatatos, K. Pringouri, T. A. Stich, K. A. Abboud, R. D. Britt, V. K. Yachandra and G. Christou, *Proc. Natl. Acad. Sci. USA*, 2012, 109, 2257-2262.
- C. Yang, S. Wang, F. Sai, D. Liu, F. Sun, Y. Gu and G. Wu, Chem. Commun., 2021, 57, 113-116.
- Y. Mousazade, M. R. Mohammadi, R. Bagheri, R. Bikas, P. Chernev, Z. Song, T. Lis, M. Siczek, N. Noshiranzadeh, S. Mebs, H. Dau, I. Zaharieva and M. M. Najafpour, *Dalton Trans.*, 2020, 49, 5597-5605.
- 25. H. B. Lee and T. Agapie, *Inorg. Chem.*, 2019, **58**, 14998-15003.
- 26. T. Ghosh, G. Christou and G. Maayan, *Angew. Chem. Int. Ed.*, 2019, **58**, 2785-2790.

- M. Yagi, K. V. Wolf, P. J. Baesjou, S. L. Bernasek and G. C. Dismukes, *Angew. Chem. Int. Ed.*, 2001, **40**, 2925-2928.
- W. F. Ruettinger and G. C. Dismukes, *Inorg. Chem.*, 2000, 39, 1021-1027.
- A. I. Nguyen, M. S. Ziegler, P. Oña-Burgos, M. Sturzbecher-Hohne, W. Kim, D. E. Bellone and T. D. Tilley, *J. Am. Chem. Soc.*, 2015, 137, 12865-12872.
- 30. F. Evangelisti, R. Moré, F. Hodel, S. Luber and G. R. Patzke, *J. Am. Chem. Soc.*, 2015, **137**, 11076-11084.
- S. Berardi, G. La Ganga, M. Natali, I. Bazzan, F. Puntoriero, A. Sartorel, F. Scandola, S. Campagna and M. Bonchio, J. Am. Chem. Soc., 2012, 134, 11104-11107.
- F. Song, R. Moré, M. Schilling, G. Smolentsev, N. Azzaroli, T. Fox,
 Luber and G. R. Patzke, J. Am. Chem. Soc., 2017, 139, 14198-14208.
- 33. J. Lin, X. Liang, X. Cao, N. Wei and Y. Ding, *Chem. Commun.*, 2018, **54**, 12515-12518.
- X. Jiang, J. Li, B. Yang, X.-Z. Wei, B.-W. Dong, Y. Kao, M.-Y. Huang, C.-H. Tung and L.-Z. Wu, *Angew. Chem. Int. Ed.*, 2018, 57, 7850-7854.
- 35. J.-H. Xu, L.-Y. Guo, H.-F. Su, X. Gao, X.-F. Wu, W.-G. Wang, C.-H. Tung and D. Sun, *Inorg. Chem.*, 2017, **56**, 1591-1598.
- P. F. Smith, C. Kaplan, J. E. Sheats, D. M. Robinson, N. S. McCool,
 N. Mezle and G. C. Dismukes, *Inorg. Chem.*, 2014, 53, 2113-2121
- J. Deutscher, T. Corona, K. Warm, X. Engelmann, S. Sobottka, B. Braun-Cula, B. Sarkar and K. Ray, *Eur. J. Inorg. Chem.*, 2018, 2018, 4925-4929.
- J. S. Kanady, J. L. Mendoza-Cortes, E. Y. Tsui, R. J. Nielsen, W. A. Goddard and T. Agapie, J. Am. Chem. Soc., 2013, 135, 1073-1082
- 39. S. Mauthe, I. Fleischer, T. M. Bernhardt, S. M. Lang, R. N. Barnett and U. Landman, *Angew. Chem. Int. Ed.*, 2019, **58**, 8504-8509.
- 40. S. Vaddypally, S. K. Kondaveeti, J. H. Roudebush, R. J. Cava and M. J. Zdilla, *Chem. Commun.*, 2014, **50**, 1061-1063.
- 41. M. R. Gau, C. R. Hamilton and M. J. Zdilla, *Chem. Commun.*, 2014, **50**, 7780-7782.
- 42. C. R. Hamilton, M. R. Gau, R. A. Baglia, S. F. McWilliams and M. J. Zdilla, *J. Am. Chem. Soc.*, 2014, **136**, 17974-17986.
- 43. C. Zhang, C. Chen, H. Dong, J.-R. Shen, H. Dau and J. Zhao, *Science*, 2015, **348**, 690-693.
- 44. S. Mukhopadhyay, S. K. Mandal, S. Bhaduri and W. H. Armstrong, *Chem. Rev.*, 2004, **104**, 3981-4026.
- W.-F. Xie, L.-Y. Guo, J.-H. Xu, M. Jagodič, Z. Jagličić, W.-G. Wang, G.-L. Zhuang, Z. Wang, C.-H. Tung and D. Sun, *Eur. J. Inorg. Chem.*, 2016, 3253-3261.
- 46. B. D. Murray and P. P. Power, *Inorg. Chem.*, 1984, **23**, 4584-
- S. Vaddypally, I. G. McKendry, W. Tomlinson, J. P. Hooper and M. J. Zdilla, *Chem.–Eur. J.*, 2016, 22, 10548-10557.
- C. G. Werncke, E. Suturina, P. C. Bunting, L. Vendier, J. R. Long, M. Atanasov, F. Neese, S. Sabo-Etienne and S. Bontemps, Chem.-Eur. J., 2016, 22, 1668-1674.
- 49. J. J. Ellison, P. P. Power and S. C. Shoner, *J. Am. Chem. Soc.*, 1989, **111**, 8044-8046.
- 50. M. A. Putzer, B. Neumüller, K. Dehnicke and J. Magull, *Chem. Ber.*, 1996, **129**, 715-719.
- 51. A. Boussac and A. W. Rutherford, *Biochim. Biophys. Acta-Bioenerg.*, 2000, **1457**, 145-156.
- 52. K. Xu, Chem. Rev., 2004, 104, 4303-4417.